

# An instrument for internal surface analysis of LEP 200 Superconducting Radiofrequency Cavities

D. Lacarrère, C. Benvenuti, R. Cosso, G. Foffano, J. Genest, M. Hauer,  
D. Jegou, D. Latorre, I. Magnani, A. Rijllart, R. Saban, F. Scalambryn  
CERN, 1211 Geneva 23, Switzerland

## *Abstract*

The LEP energy upgrade program at CERN requires the use of 192 superconducting (SC) radiofrequency (RF) cavities which will be progressively installed in the LEP collider. The industrial production of SC cavities is presently being carried out by three European contractors. Contamination and defects which may be generated during both the manufacturing process and the setting up of the components may have detrimental effects on the radiofrequency performance and the reliability of the SC accelerating cavities. To obtain a better understanding of the origin and nature of these defects, a diagnostic tool, based on a computer controlled surface analysis instrument providing Secondary Electron Microscopy (SEM) imaging, static Auger Electron Spectroscopy (AES) and Scanning Auger Mapping (SAM) directly inside the cavity has been designed and built at CERN.

An overview of the project and of the technical solutions used are presented in this paper. Preliminary results are also reported.

## *1. Introduction*

The LEP energy upgrade program at CERN requires the use of 192 superconducting (SC) radiofrequency (RF) cavities which will be installed progressively in the LEP collider [1]. The industrial production of SC cavities is presently being carried out by three European contractors. About 170 of these cavities will be made from copper sheet, internally coated with a thin layer of Nb (approximately 1 $\mu$ m thick) deposited by magnetron sputtering [2, 3]. Contamination and defects which may be generated during both the manufacturing process and the setting up of the RF ancillary equipment have adverse effects on the radiofrequency performance and the reliability of the SC cavities [4, 5]. Therefore, information about the morphology, size, distribution, quantity and elemental composition of impurities and defects should provide invaluable help in guiding and improving the ongoing industrial production.

For this reason, during the last decade various diagnostic techniques have been developed such as Scanning Thermography [6, 8], Scanning Electron Microscopy [9] and Field Emission Scanning Microscopy [10]. However, a direct link between the nature of the local surface defects and/or contamination and their effects on the RF operating conditions is still lacking. In order to bridge this gap in our understanding, a new diagnostic tool, hereafter called "Strombinoscope", based on a computer controlled surface analysis instrument, has been built at CERN and is presented here. It combines Secondary Electron Microscopy (SEM), static Auger Electron Spectroscopy (AES) and Scanning Auger Mapping (SAM) measurements to be performed directly inside a SC 352 MHz 4-cell cavity. This instrument allows the inspection and analysis of defects on the inner cavity surface, previously localised by temperature mapping during RF measurements. The information obtained may provide the key to the understanding of the origin of the defects and may also provide some further insight into the mechanism of electron field emission.

## 2. Design and construction considerations

### 2.1 General design

The "Strombinoscope" can be regarded as the ensemble of two systems, mounted vertically, separated by a 200 mm inner diameter UHV gate valve (Fig. 1). The upper part consists of a manifold incorporating pumps and gauges, to which an RF cavity can be attached. The lower part consists of a computer controlled robot arm, supporting the analysis instrument, mounted on a stage permitting both z axial translation between the lower and upper system and  $\Phi$  rotation, and providing the necessary UHV housing. The specifications of the apparatus described below are given in Table 1.

The gate valve is used to separate the vacuum in the two systems, making it possible to change the cavity under investigation without venting the lower chamber. Both systems are equipped with a 200 l/s turbomolecular pump, a 60 l/s sputter ion pump and a non evaporable lumped getter pump, which is activated by passive heating at 300 °C for an hour [11] with pumping speed for hydrogen of about 2000 l/s. An RF cavity, transported under inert gas atmosphere, is installed on the manifold and pumped to UHV using the upper chamber pumps. Several pressure gauges, namely 2 Pirani gauges, 2 Penning gauges, 3 Bayard-Alpert gauges and 2 mass spectrometers, provide a vacuum status of each separate system. Once UHV is achieved in the RF cavity, the gate valve can be opened to allow the analysis instrument on the robot arm to pass from the lower chamber into the cavity. The z translation is achieved by the motion of the z-translational stage using a computer controlled stepping motor. This motion is permitted through the compression of the bellows enclosing the robot arm and the analysis instrument. The z translation, together with the tilt  $\alpha$  and the rotation  $\Phi$  of the analytical head, similarly achieved through computer controlled stepping motors, allow surface analysis of the upper hemispheres of the RF cavity under investigation. The tilt motion is achieved by a simple rack and pinion mechanism. A maximum tilt angle of 74° from the vertical direction is obtainable, restricted by the head mounting bellows (see Fig. 2) which separate the cabling from the UHV environment of the instrument.

It should be noted here that it is possible to analyse the equatorial region of the cavity through a suitable combination of  $\alpha$  and  $z$  motions.

The  $\Phi$  motion is achieved through three differentially pumped Viton O-rings, situated at the bottom of the robot arm, ensuring good vacuum under operation. Appropriate absolute encoders allow positioning on the area on the cavity surface which has been selected by the operator for surface analysis.

The standard SC cavity analysis procedure can be summarised as follows : the robot control software moves the analytical head inside the cavity on a virtual 3-D surface which is situated, on average, at a distance of about 10 mm from the SC cavity surface, the exact distance depending on the precise cavity geometry. The software is capable of positioning the head on a point chosen by the operator in the upper cells of the cavity on the ideal surface (Fig. 2). Fine positioning of the analytical head is achieved with the aid of specular beam calibration. The areas of interest for the surface analysis of each SC cavity are pre-determined following the results of temperature mapping measurements which provide an indication of the spatial position of defects on the cavity surface. The analysis takes place in a strict order; first the lowest cell, proceeding to the highest, analysing the upper portion of each cell. This procedure reduces the risk of contamination induced by particles falling from the instrument itself during the measurements. In order to analyse the lower part of the four cells, i.e. for a complete analysis of the cavity internal surface, the cavity has to be dismantled, rinsed, remounted in the opposite sense and the analysis procedure repeated. The vertical mounting of the "Strombinoscope" was chosen not only for this reduced risk of cavity contamination by the instrument during the measurement, but also to provide better mechanical stability.

## ***2.2 Robot arm control software and interlock system***

The three-axis robot arm, which carries the analytical head, is controlled via a Personal Computer (PC) which hosts a controller card and runs a Visual Basic application [12]. The block diagram of the control system is shown in Fig. 3. This application provides a user interface by visualizing the position of the analytical head inside the cavity and executing acceptable move commands. It also serves as equipment interface between the PC and the stepping motor controller.

The 4-cell cavity shape has been pre-defined, but small geometrical imperfections can be accommodated for in the form of a few parameters entered by the user.

Software protections have been made to avoid a collision between the analytical head and the cavity wall.

A hardware interlock system has been made to provide further protection against analytical head and cavity collision and other undesirable events, such as opening the separation gate valve with bad vacuum in the cavity or closing it with the head still inside the cavity.

It consists of a Programmable Logic Controller (PLC) which receives its inputs from limit switches, vacuum gauges and a head inclination sensor to avoid collision under practically all circumstances and a mechanical force sensor to limit the damage in the unlikely event of a collision.

A switch panel with a synoptic diagram shows the state of the interlock system and allows users to reset error conditions. The interlock status can also be visualised on the PC through separate inputs on the controller card.

### **3. Surface analysis system**

Auger Electron Spectroscopy (AES), Scanning Auger Mapping (SAM) and Secondary Electron Microscopy (SEM) [13] are used here in order to perform both elemental and topographical analysis of the SC cavities. AES makes it possible to identify and quantify, at the microscopic level, all elements present in the few outer atomic levels of a material (except H and He). Secondary electron images provide detailed topographical information. They are obtained by rastering a focused electron beam across the surface of a specimen and collecting, here with a channeltron electron multiplier detector, the secondary electrons emitted in the process. Combining this information with Auger line scans and chemical maps it is possible to identify both the nature of the constituents and their location on the sample.

In order to perform AES and SAM analyses a single pass cylindrical mirror analyser (CMA) with coaxial electron gun manufactured by PHI Perkin-Elmer, model 15-110B, was chosen. The Secondary Electron Detector (SED) for SEM is also produced by PHI and simply consists of a channeltron electron multiplier with related electronics.

To adapt the CMA and SED on the robot arm, important hardware modifications had to be made. The modified head is shown in Figs. 2 and 4. The main modifications can be summarized as follows :

- a) The flange to target distance was reduced to 270 mm by modifying the mounting ring support and the  $\mu$ -metal shield;
- b) The original PHI mounting flange was replaced with a home-made flange enabling both the SED and the CMA to be mounted together with a sputter ion gun for surface cleaning, which will be added later if necessary;
- c) In order to perform steps a) and b), the internal connections of the CMA had to be completely recabled; also the external cabling had to be modified, so as to allow relatively easy mounting of the analytical head on the robot arm;
- d) The analyser relative energy resolution  $\Delta E/E$  was fixed to 1.2% by mechanically setting the variable entrance slit on the corresponding aperture;
- e) The SED preamplifier was repackaged in order to insert it in the tube as close as possible to the detector.

The characteristics of the analysis instrument are summarised in Table 2. Following these major modifications, the CMA and SED ensemble was mounted on a standard vacuum chamber in order to verify its correct operation.

The final assembly of the system in the configuration shown in Fig. 2 was then carried out. In order to allow evaluation of the spatial resolution of the system and to provide reference samples for the Auger analysis, an Au specimen, a Cu specimen and a Cu plated grid with mesh of 25  $\mu\text{m}$  pitch and bar width of 6  $\mu\text{m}$ , were placed on a retractable sample holder mounted on the instrument chamber.

#### **4. Preliminary results**

Preliminary results obtained on a Nb coated cavity are shown in Figs. 5 to 8. In Fig. 5 a typical AES spectrum of a Nb coated cavity is presented. C and O contamination of the Nb layer is clearly observed as expected, due to cavity exposure to the atmospheric pressure. In Fig. 6 two photographs of typical SED images of defects observed on the cavity surface during the calibration run are displayed. The C and O Auger maps corresponding to Fig. 6 A are shown in Fig. 7.

The dark zones correspond to higher concentration of the detected element. Nb maps were also acquired on the same area and they did not show the same dark spot at the bottom-centre of the image that clearly appears on the C and O maps.

Since no other elements than C, O and Nb were detected in this region with AES area scans, it can be concluded that the observed defect consists of carbon or of carbonaceous compounds. Finally, Fig. 8 shows the C and O line scans corresponding to the defect of Fig. 6 B. The peak in Fig. 8 a corresponds to high oxide concentration on the defect. These results indicate that the instrument provides valuable information on the elemental composition of cavity surface defects.

#### **5. Concluding remarks**

The decision to build the "Strombinoscope" instrument was taken at the beginning of 1992. The construction and commissioning were accomplished in about 1 year. The performance reached so far (lateral resolution  $\sim 10 \mu\text{m}$  @ 3.5 kV) is very close to the specified performance ( $\leq 3 \mu\text{m}$  @ 10 kV). Preliminary results obtained from an *in situ* examination of a Nb-coated Cu cavity are extremely encouraging and the capabilities of the instrument are clearly demonstrated. However, the optimization of operating parameters, to achieve a better signal-to-noise ratio, has not been carried out yet. Electromagnetic interferences, due to the close proximity of the  $\alpha$  stepping motor cabling and the SED preamplifier cabling in the central tube, must be reduced in order to improve the quality of SED images. Other future improvements are planned, such as, for example, the addition of a sputter ion gun which could allow depth profiling and possibly defect removal.

#### **6. Acknowledgements**

The authors are indebted to J. P. Biberian (International Consultant) and L. E. Davis (Technical Support Manager, Perkin Elmer, Physical Electronics Division) for discussions and invaluable advice at the early stages of the project.

C. Wyss and Ph. Bernard (CERN) are also gratefully acknowledged for supporting and funding this project.

## References

- [1] C. Wyss, CERN AC/93-02 (LEP200), PAC93 Washington D. C., May 1993.
- [2] C. Benvenuti, N. Circelli, M. Hauer, Appl. Phys. Lett. 45 (5), 1984, p. 583.
- [3] C. Benvenuti, S. Calatroni, G. Orlandi, to be published in the Proceedings of the "20th International Conference in Low Temperature Physics", Eugene, Oregon, USA, August 4-11, 1993.
- [4] D. Bloess, Proc. of 3rd Workshop on RF Superconductivity, Argonne/Illinois USA, 1987, ed. K.W. Shepard.
- [5] Ph. Bernard *et al.*, Proc. of the 11th Int. Conf. on High Energy Acc., Geneva 1980, (Birkhäuser, Basel, 1980), p 878.
- [6] G. Muller, Proc. of the 2nd Workshop on RF superconductivity, CERN/Geneva (1984).
- [7] H. Padamsee *et al.*, Proc. IEEE Part. Acc. Conference, Washington, 16-19 March 1987, p. 1824-1826.
- [8] C. E. Reece, Proc. of the 3rd Workshop on RF superconductivity, Argonne, Illinois, USA (1987), p. 545-563.
- [9] A.G. Mathewson, A. Grillot, J. Vac. Sci. Technol. 21 (3) Sept/Oct 1982, p 867-871.
- [10] P. Niedermann *et al.*, J. Appl. Phys. 59 (3), February 1986, p. 892-901.
- [11] C. Benvenuti and P. Chiggiato, Vacuum 44 (5-7) 1993, p. 511.
- [12] D. Jegou, MT-SM Note 93-04, AT Group Report 93-04 (IC), June 1993.
- [13] See, for example : "Practical Surface Analysis" second edition, Volume 1 (Auger and X-ray Photoelectron spectroscopy), edited by D. Briggs and M.P. Seah, John Wiley & Sons, 1990.

## ***Table captions***

**Table 1 : Main characteristics of the instrument.**

**Table 2 : Cylindrical Mirror Analyser and Electron Gun nominal characteristics in the modified configuration.**

## ***Figure Captions***

**Fig. 1** General layout of the "Strombinoscope" instrument.

**Fig. 2** View of the Cylindrical Mirror Analyser (CMA) and Secondary Electron Detector (SED) fitted on the robot arm inside a cell of a SC RF cavity (detail).

**Fig. 3** Block diagram of the robot.

**Fig. 4** Photographs of the analytical head mounted at the top of the inner tube; a) without bellows; b) with bellows.

**Fig. 5** Typical Auger spectrum recorded from cavity surface. The instrumental parameters that were used during the data acquisition were : Primary electron beam voltage 2.5 kV; Filament current 2.8 A; CMA channeltron HT 800 V; SED channeltron HT 1840 V; magnification 170.

**Fig. 6** Photographs of SED images of typical defects; above : defect A; below : defect B.

**Fig. 7** SAM of defect A (compare with figure 6 A); a) C map; b) O map. Darker areas correspond to higher concentration of the detected element.

**Fig. 8** Line scans of defect B (compare with figure 6 B); a) O scan; b) C scan. The increase in intensity corresponds to increase in the concentration of the detected element.

**TABLE 1**

Total length of the instrument without and with fitted cavity	6000 mm, 8410 mm
Z translation max. amplitude inside cavity, linear resolution	2650 mm, 0.1 mm
Internal tube length, diameter	5200 mm, 170 mm
Cavity access flange, internal diameter	198 mm
Outer bellows expanded and compressed length	3535 mm, 885 mm
Internal, external diameter	200 mm, 250 mm
Internal bellows length	250 mm
Internal, external diameter	150 mm, 180 mm
Alpha tilt angle range, angular resolution	0° to 74°, 0.06°
Phi rotation angle range, angular resolution	0° to 370°, 0.06°
Bakeability	up to 120°C
Typical operating pressure	$< 5.0 \times 10^{-9}$ Torr

**TABLE 2**

Analysis instrument mounting flange O.D.	180 mm
CMA modified length, diameter	275 mm, 130 mm
SED length, diameter	150 mm, 35 mm
V/F CMA preamplifier position	7000 mm from CMA
SED preamplifier position (cabling length)	1100 mm from SED
Electronic control units position	15000 mm from preamplifiers
CMA working distance	6.5 mm
Incidence angle e <sup>-</sup> beam/surface (range)	0° to 27°
Minimum electron beam diameter	$< 3 \mu\text{m}$ @ 40 nA
Maximum electron beam energy	10 keV
Maximum beam current	$> 10$ mA
Analyser relative energy resolution ( $\Delta E/E$ )	Fixed : 1.2 %
Magnification range	50 x to 5000
Smallest scanning area	$10 \times 10 \mu\text{m}^2$
Largest scanning area	$400 \times 400 \mu\text{m}^2$



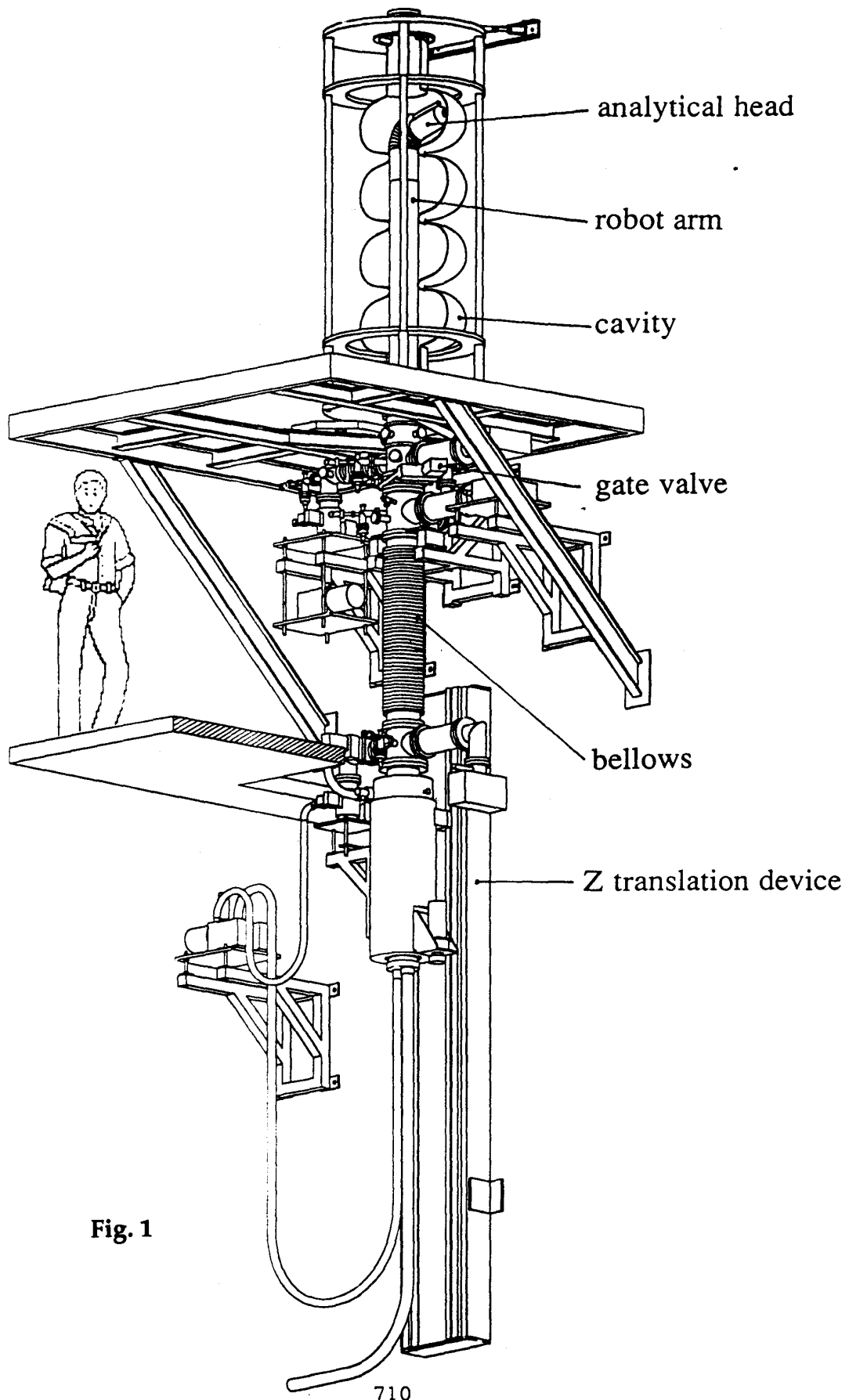
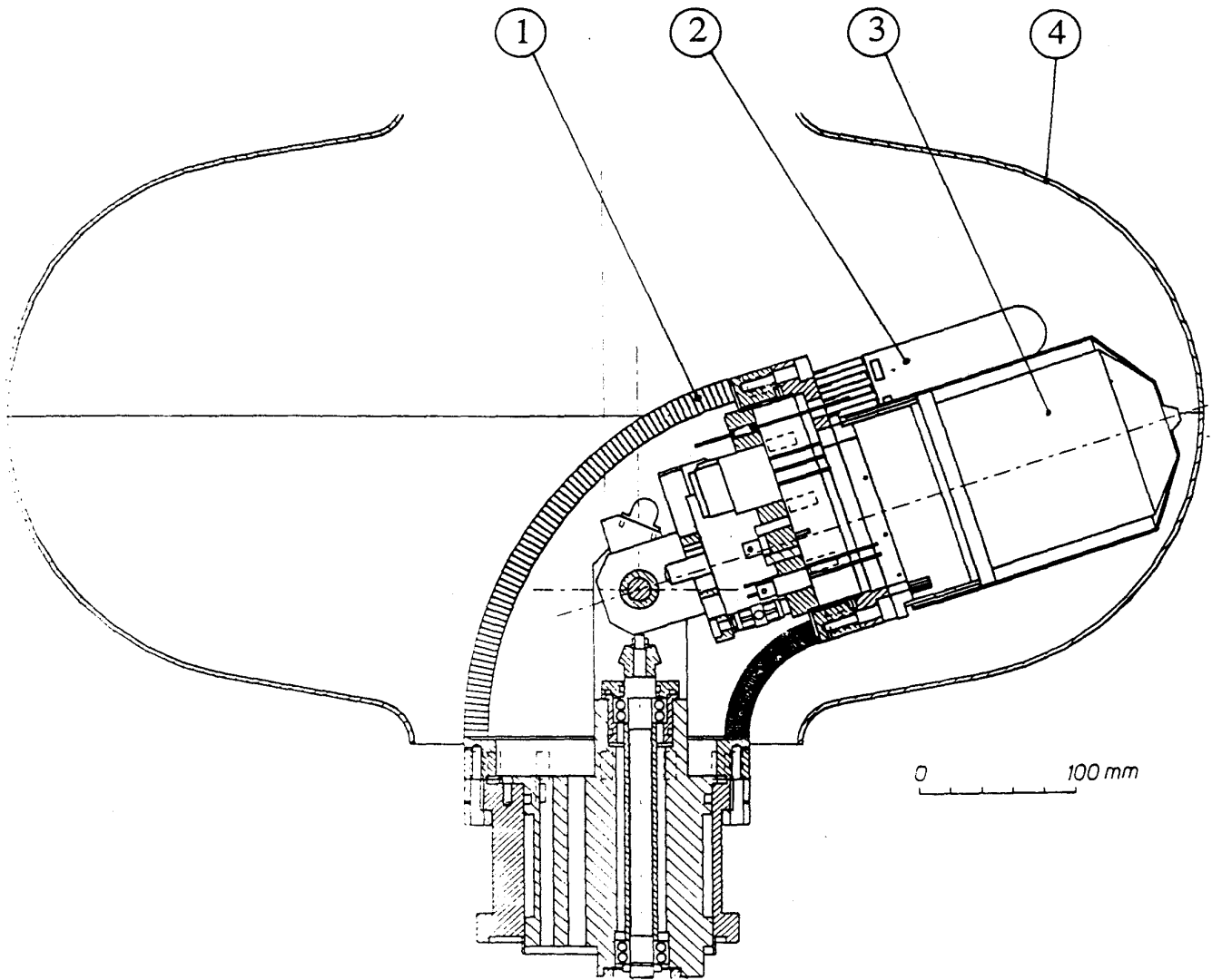


Fig. 1



- ① internal bellows
- ② SED
- ③ CMA
- ④ cavity cell

**Fig. 2**

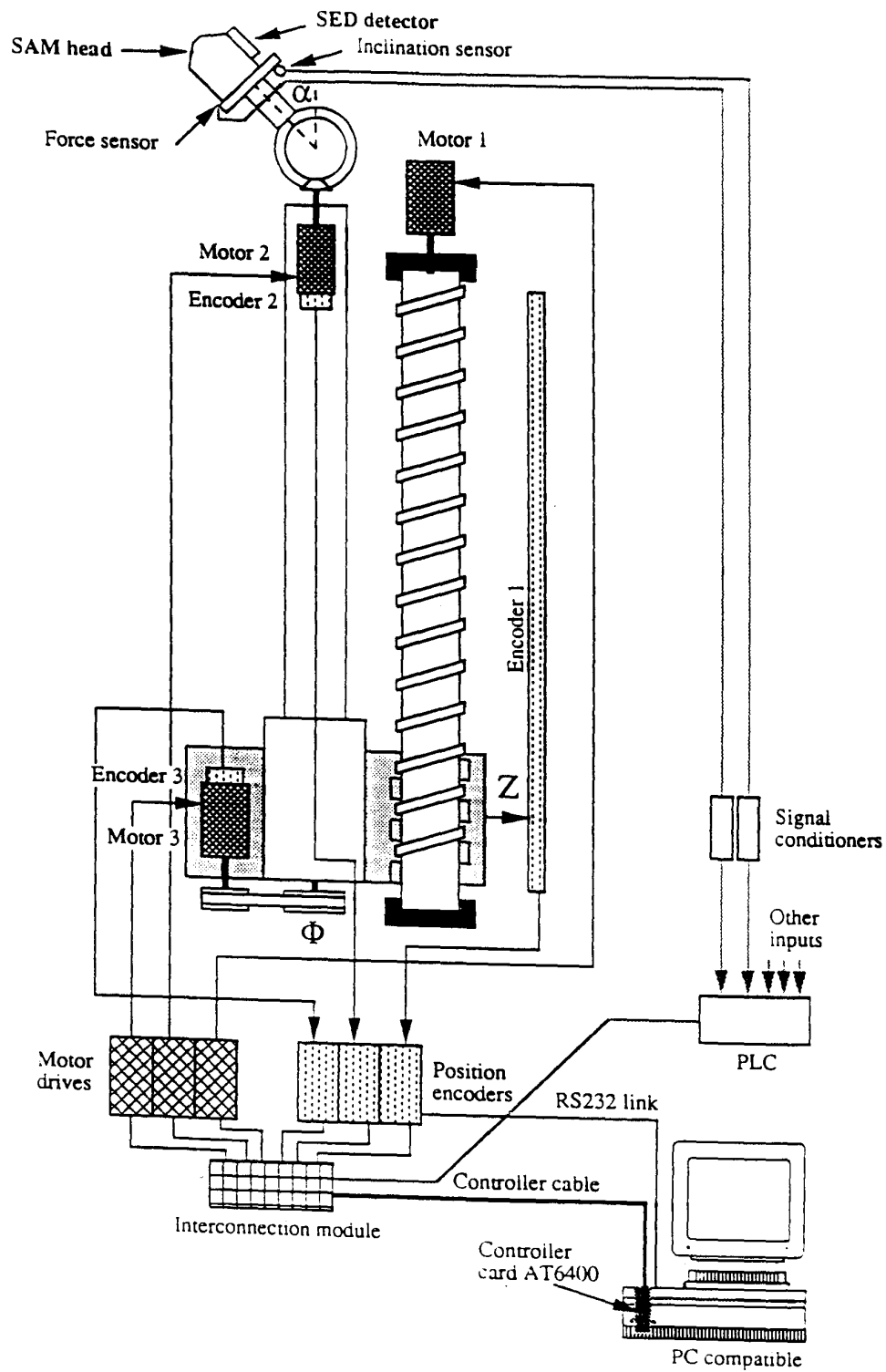
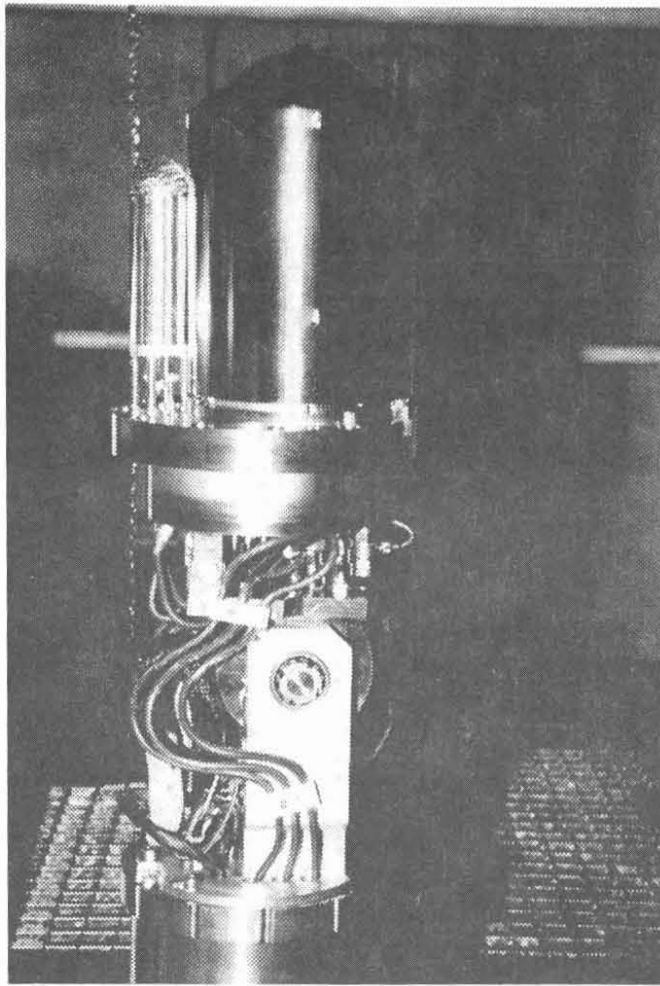
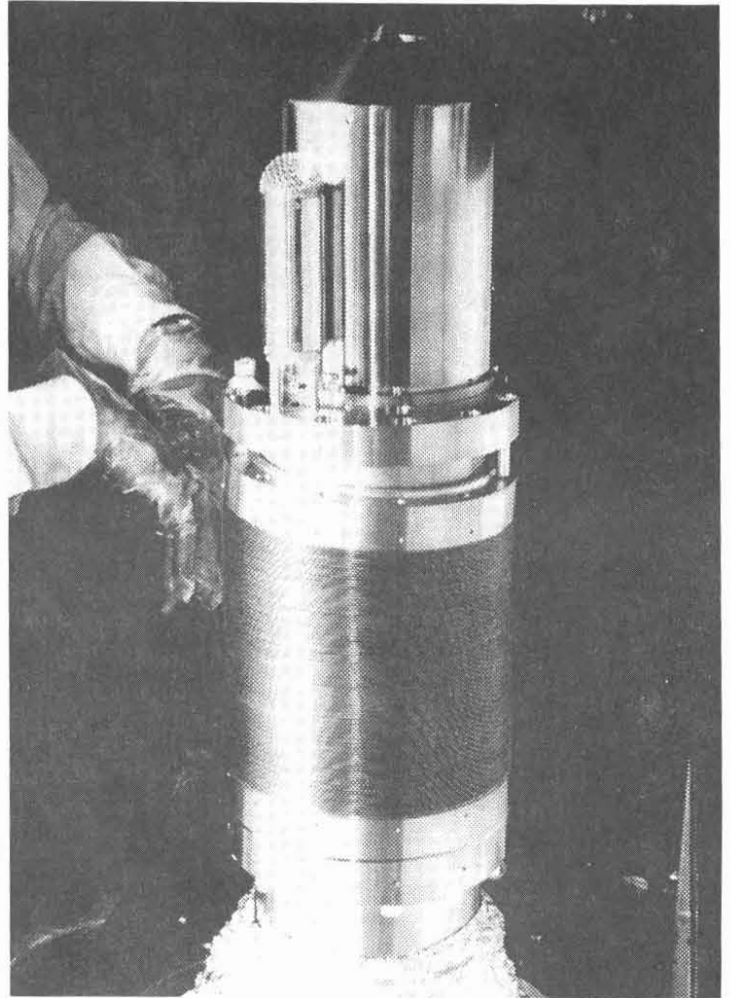


Fig. 3



a



b

Fig. 4

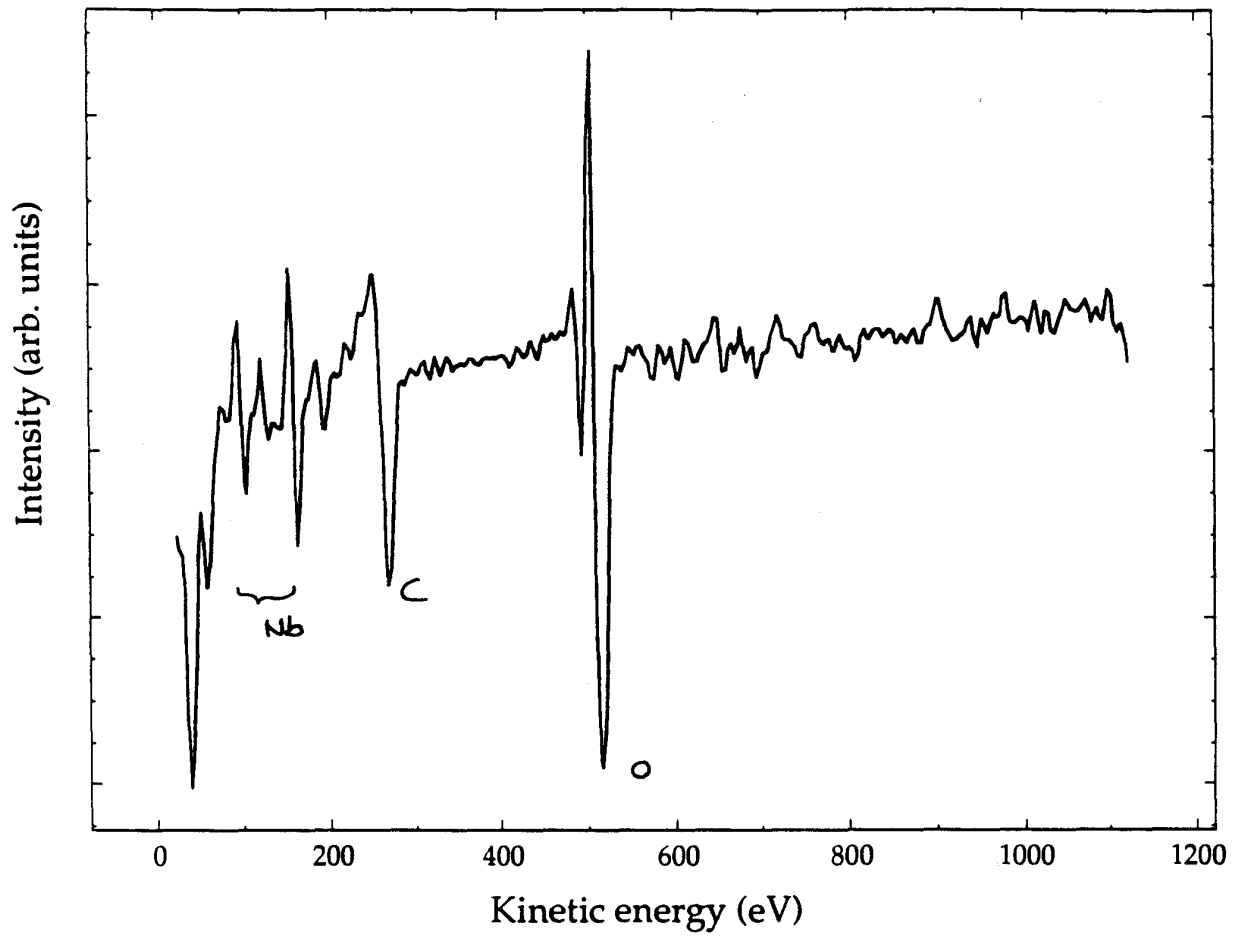
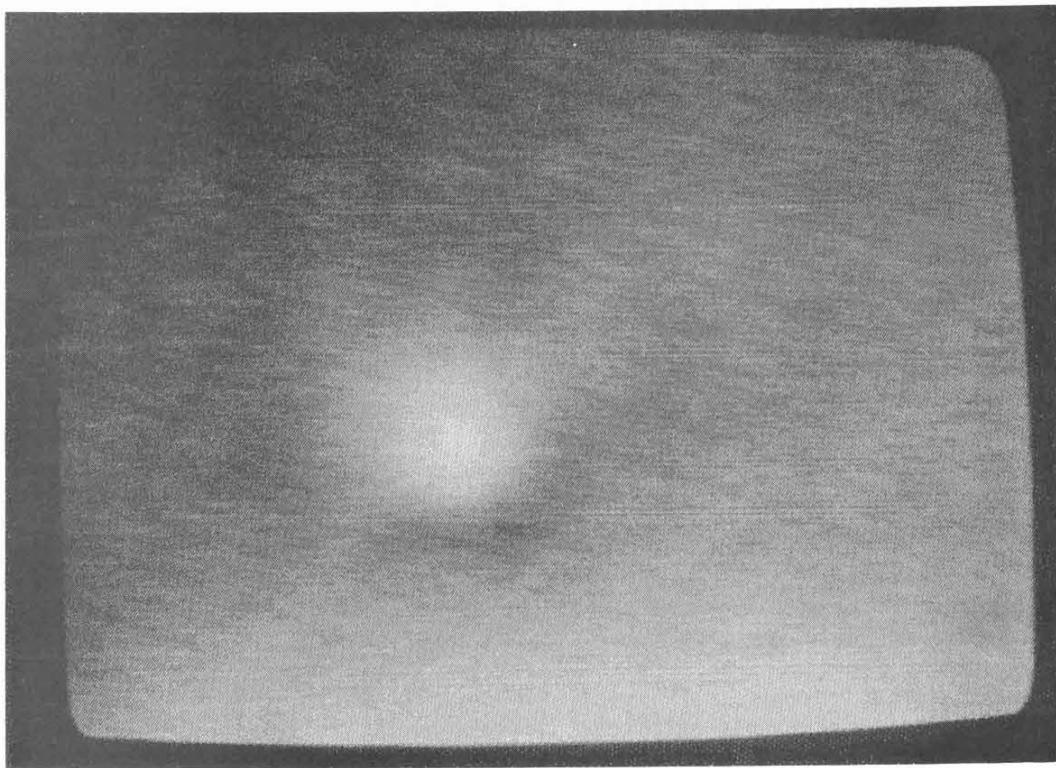
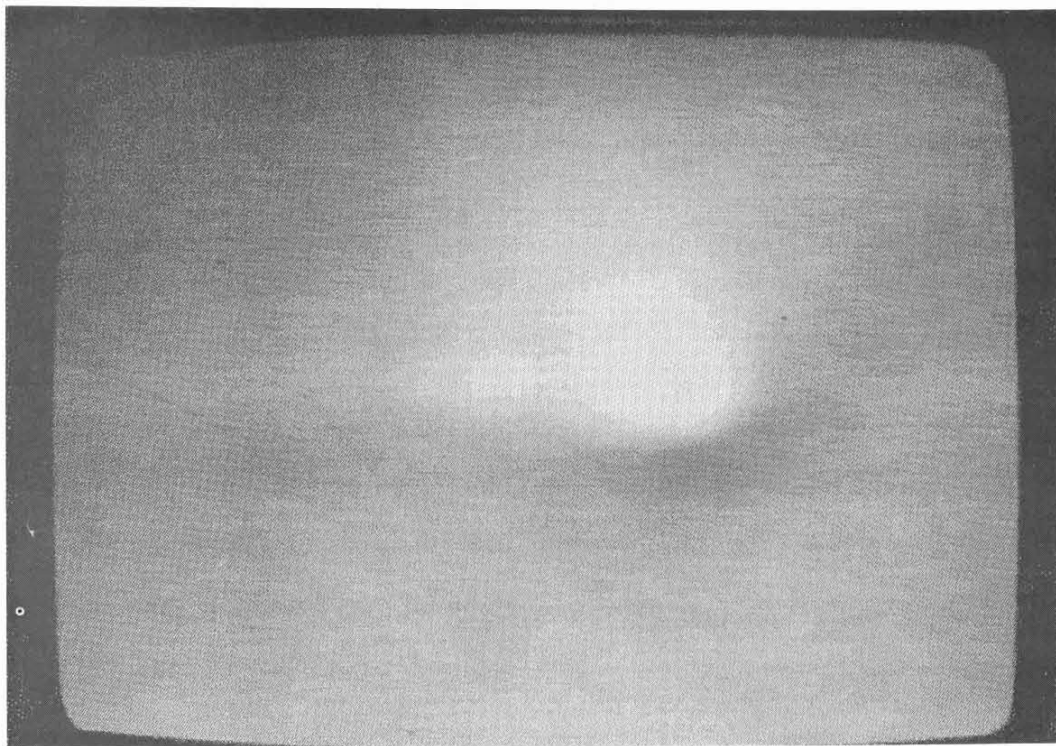


Fig. 5



A)



B)

—  
100  $\mu\text{m}$

**Fig. 6**

715

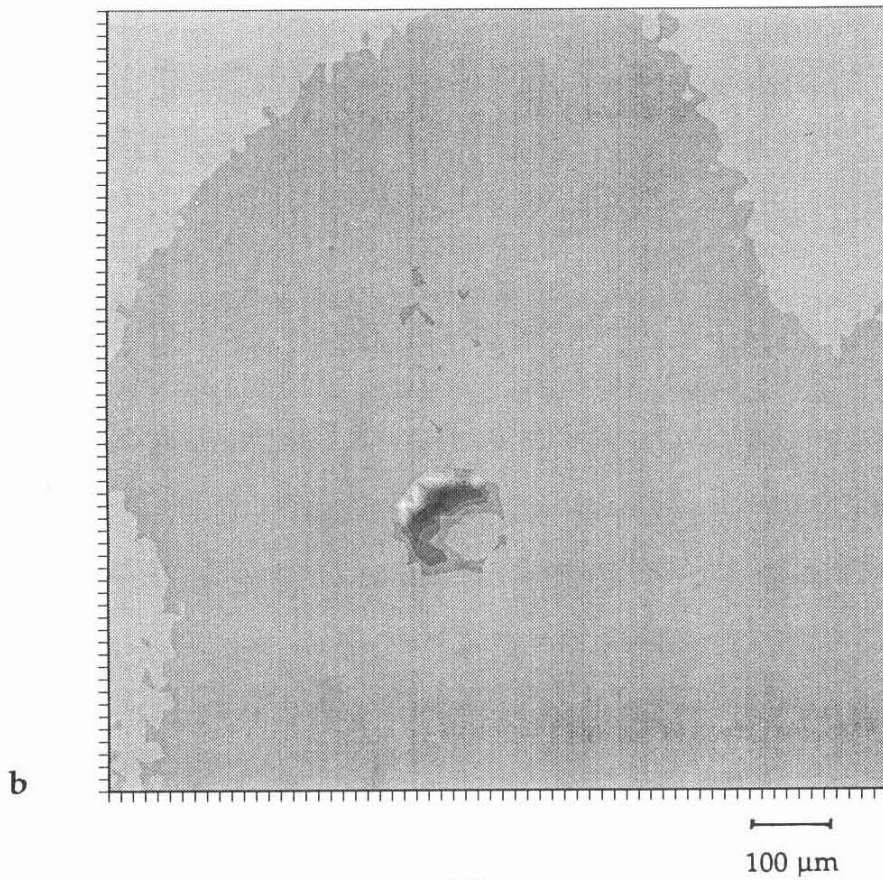
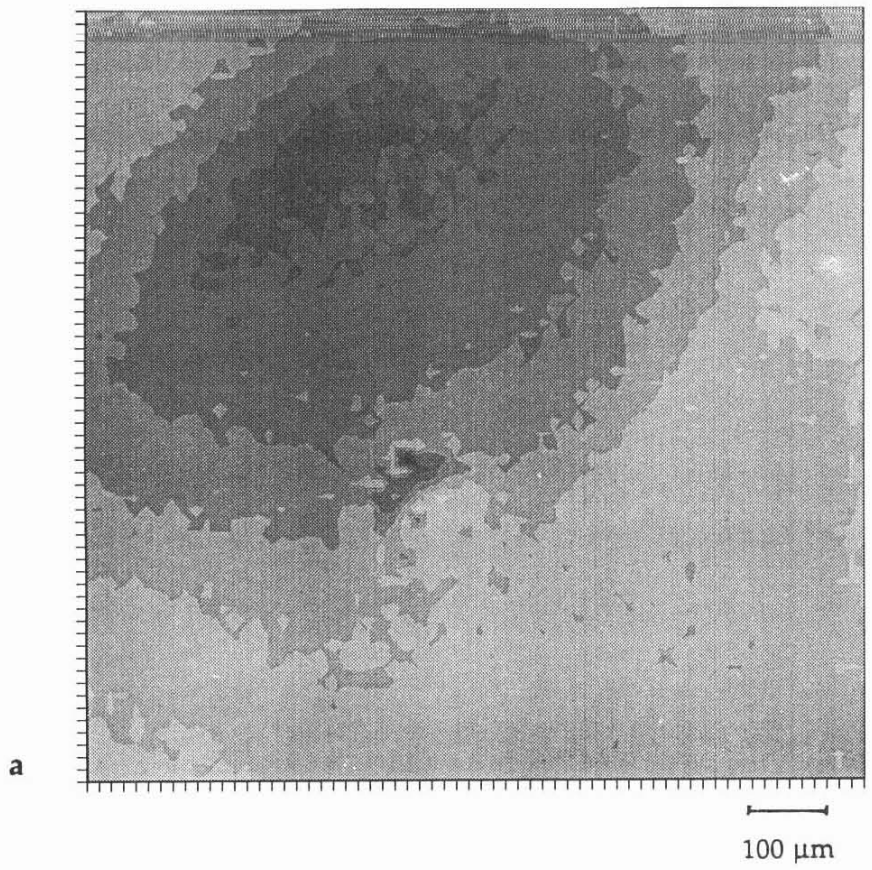


**Fig. 7**

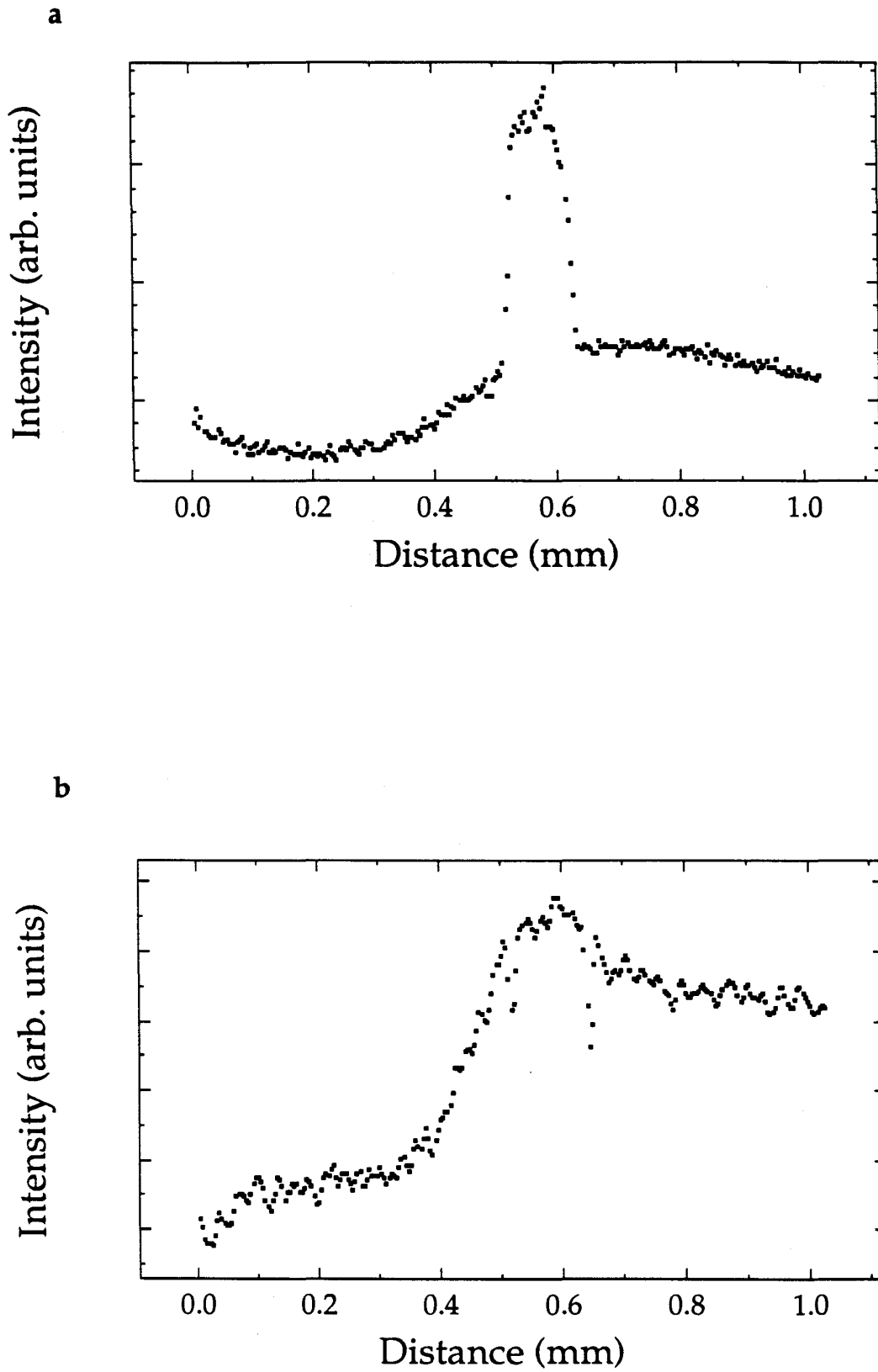


Fig. 8